TABLE 4
Input Impedance and Resonant Frequency Results for a Chosen Sample Case After Matching Via Microgenetic Algorithm, TM_{11} Mode, $d_0 = 1.27$ mm, tan $\delta = 0.001$

h_1	a (mm)	ε_r	f_r-des (MHz)	f_r-obt (MHz)	h_2 (mm)	ρ (mm)	Re (Z)	Im (Z)	SWR
1.59	50	2.32	1281	1282.2	0.507	13.80	50.16	9.73	1.21

network is required for maximum transfer of power from a coaxial line to the antenna. However, using the proposed technique, the 'patch antenna could be matched to a 50 Ω coaxial line without extra tuning circuitry. Optimization results are summarized in Table 2, where the first three columns give samples for different structural parameters while the fourth and fifth columns give the optimized gap thickness h_2 and coaxial feed position ρB on the patch to provide the desired matching. It is observed from Table 2 that for all cases, the specifications on the resonant frequency and input impedances are well satisfied. SWR of each case reach the acceptable SWR value range of 1.2–2.0.

Input impedance and resonant-frequency results for a sample case ($h_1 = 1.59$ mm, $a = 50$ mm, $\varepsilon_r = 2.32$, TM_{11} mode) are given in Tables 3 and 4. Before tuning, resonant frequency of double-layered circular patch microstrip antenna is 1281 MHz, and the corresponding input impedance and SWR values are $318 - j0.32$ Ω and 6.36, respectively. After the adjustment of the air gap thickness and the coaxial feed position, SWR is reduced to 1.21 at the resonant frequency of 1282.2 MHz; the corresponding input impedance is around $(50.16 + j9.73)$ Ω. Since the input resistance of the antenna without matching network is now near 50 Ω at predetermined resonant frequency, maximum power is transferred to the antenna.

6. CONCLUSION

In this study, simple and accurate resonant frequency and input impedance calculations of a coaxial fed, double-layered circular patch microstrip antenna, are performed using new radius extension formula and effective permittivity expression including modal effects. For both cases, improved accuracy is obtained with respect to the previously published results in literature for various cases. Input impedance matching approach proposed in the last part of the study depending on the usage of microgenetic algorithm is also verified with satisfactory results obtained within small computational time. The given expressions in this study for effective patch radius and the effective permittivity can also be used in the calculations of other operational characteristics of the same antenna in future studies.

REFERENCES

1. K.F. Lee, K.Y. Ho, and J.S. Dahele, Circular disk microstrip antenna with an air gap, IEEE Trans Antennas Propag 32 (1984), 880–884.
2. J.S. Dahele and K.F. Lee, Theory and experiment on microstrip antennas with air gap, Proc IEE 132 (Part H) (1985), 455–460.
3. F. Abboud, J.P. Damiano, and A. Papiernik, A new model for calculating the input impedance of coax-fed circular microstrip antennas with and without air gap, IEEE Trans Antennas Propag 38 (1990), 1882–1885.
4. J.S. Joy and B. Jecko, A formula for the resonance frequencies of circular microstrip patch antenna satisfying CAD requirements, Int J RF Microwave Comp Aided Eng 3 (1993), 67–70.
5. K. Guney, Resonant frequency of electrically-thick circular microstrip antenna, Int J Electron 77 (1994), 377–385.
6. Ç.S. Gurel and E. Yazgan, Modified resonant frequency calculation for two-layered circular patch microstrip antenna, AEU-Int J Electron Commun 53 (1999), 155–157.
7. Ç. S. Gurel and E. Yazgan, New determination of dynamic permittivity and resonant frequency of tunable circular disk microstrip structures, Int J RF Microwave Comp Aided Eng 10 (2000), 120–126.
8. Ç.S. Gurel and E. Yazgan, Resonant frequency of an air gap tuned circular disk microstrip antenna, Int J Electron 87 (2000), 973–979.
9. D. Guha, Resonant frequency of circular microstrip antennas with and without air gaps, IEEE Trans Antennas Propag 49 (2001), 55–59.
10. T. Gunel, Continuous hybrid approach to the modified resonant frequency calculation for circular microstrip antennas with and without air gaps, Microwave Opt Tech Lett 40 (2004), 423–427.
11. O. Ozgun, S. Mutlu, M.I. Aksun, and L. Alatan, Design of dual-frequency probe-fed microstrip antennas with genetic optimization algorithm, IEEE Trans Antennas Propag 51 (2003), 1947–1954.
12. Y. Rahmat-Samii and E. Michielssen (Eds.), Electromagnetic optimization by genetic algorithms, New York, Wiley, 1999.
13. J.Y. Siddiqui and D. Guha, Improved formulas for the input impedance of probe-fed circular microstrip antenna, IEEE Int Symp Dig 3, Columbus, OH (2003), 152–155.
14. S.D. Rogers, C.M. Butler, and A.Q. Martin, Design and realization of GA-optimized wire monopole and matching network with 20:1 bandwidth, IEEE Trans Antennas Propag 51 (2003) 493–502.
15. D.L. Carroll, Program GA FORTRAN, Department of Mechanical Engineering, University of Illinois, Urbana, 1997.

RETROFITTABLE ANTIREFLECTION COATINGS FOR T-RAYS

Withawat Withayachumnankul, Bernd M. Fischer, Samuel P. Mickan, and Derek Abbott
School of Electrical & Electronic Engineering, The University of Adelaide, Adelaide, SA 5005, Australia

Received 13 February 2007

ABSTRACT: *T-ray reflection loss at a window's surface is reduced by means of a quarter-wave antireflection coating. Because T-ray wavelengths are much longer than visible wavelengths, the antireflection layer for T-rays is much larger than the layers typically used in optics. This creates an interesting opportunity for retrofittable antireflection layers. In the experiment, an antireflection coating made from ordinary polyethylene sheets is pressed onto the surfaces of a silicon window in the way that rapid replacement of the rettrofittable coating is possible. Measured by terahertz time-domain spectroscopy (THz-TDS), the coated window shows enhancement of the transmittance within a range of T-ray frequencies.* © 2007 Wiley Periodicals, Inc. Microwave Opt Technol Lett 49: 2267–2270, 2007; Published online in Wiley InterScience (www.interscience.wiley.com). DOI 10.1002/mop.22664

Key words: *antireflection coating; T-rays; terahertz; THz-TDS*

1. INTRODUCTION

Terahertz time-domain spectroscopy (THz-TDS) [1] enables extraction of optical or dielectric properties of materials, whether in the solid, liquid, or gas phase, in the T-ray frequency region (≈0.1–10 THz). Spectroscopy of a liquid or gas often requires a receptacle to confine the sample. In order to allow T-rays to probe

the sample effectively, the receptacle needs T-ray transparent windows [2]. However, even though the windows are transparent to T-rays, the attenuation exists because of multiple reflections at air–window and window–air interfaces, which account for a major energy loss. This motivates the need for antireflection windows.

Because of the recent emergence of T-ray technology, there has been very little work carried out to-date on T-ray antireflection. It would appear that almost all previous research addressed the designs and analyses of antireflection windows in the mid T-ray frequency region [3, 4], i.e. from 1.5 THz to tens of terahertz. However, these designs are inappropriate for modern ultrafast T-ray systems, which operate in the frequency range of 0.1–2.0 THz or higher [1].

This work presents a quarter-wave antireflection coating, by which the window transmittance is increased for selected T-ray frequencies in between 0.1 and 1.0 THz. A thick coating of the order of ten microns allows construction of a retrofittable antireflection coating, i.e. the coating thickness can be changed rapidly to accommodate a particular frequency range. After construction, the structure is characterized by THz-TDS, which delivers the time-resolved electric field of a broadband pulse containing T-ray frequencies. To the best knowledge of the authors, this work is the first to intensively study an antireflection coating in this frequency range.

2. QUARTER-WAVE ANTIREFLECTION COATING

In the analysis, the coating material's thickness and index of refraction are represented by l_a and n_a, respectively, and the window's index of refraction by n_s. The window is assumed to be semi-infinite so that the reflection from the back surface is omitted. Through the characteristic matrix method, the optimum coating parameters, l_a and n_a, required for zero reflectance at a particular frequency, f_c, and its odd harmonics, are given by [5], $n_a = n_s^{1/2}$ and $l_a = c/(4\, n_a f_c)$.

It should be noted that the thickness condition can be rewritten in terms of the optical thickness as $n_a l_a = c/(4f_c) = \lambda_c/4$. The optical thickness of a coating layer is a quarter of the selected wavelength, resulting in a *quarter-wave antireflection coating*.

The effect of a quarter-wave antireflection coating can be visualized as follows. When the field traveling in a low-index layer is reflected off by a higher-index layer, its phase is shifted by 180°, or a half wavelength. In case of antireflection window, where $1 < n_a < n_s$, the field reflected at either the air–coating or coating–window interface will have a half wavelength phase shift. The field traversing the quarter-wave coating layer back and forth will have an additional phase shift of a half wavelength, resulting in a full wavelength phase shift, when it re-emerges into the air. The field reflected from the air-coating interface with a half wavelength phase shift will then destructively interfere with the field reflected from the coating-window interface with a full-wavelength phase shift.

3. EXPERIMENTS

In the experiment a high-resistivity silicon wafer ($n = 3.418$) is used as window due to its transparency to T-rays. For the perfect transmittance, a coating material should have the index of refraction, n_a, of $3.418^{1/2} = 1.85$. However, an ordinary material with the closest index is a series of polymers, which has the index of ~1.5. This discrepancy is tolerable with a slightly lower antireflection performance, provided the optical thickness still satisfies the quarter-wave condition.

Since the thickness of an antireflection coating for T-rays is in the order of tens of microns, it is possible to use a common polyethylene (PE) bag, which has a thickness ranging from ten to a hundred microns and is tranparent to T-rays. Use of a pre-made polyethylene film as a window coating not only avoids a complex material deposition technique, but also opens up the possibility for retrofittable and interchangeable antireflection layers in T-ray systems. During a T-ray experiment, the window coating thickness can be rapidly changed to enhance the transmittance of desired frequencies.

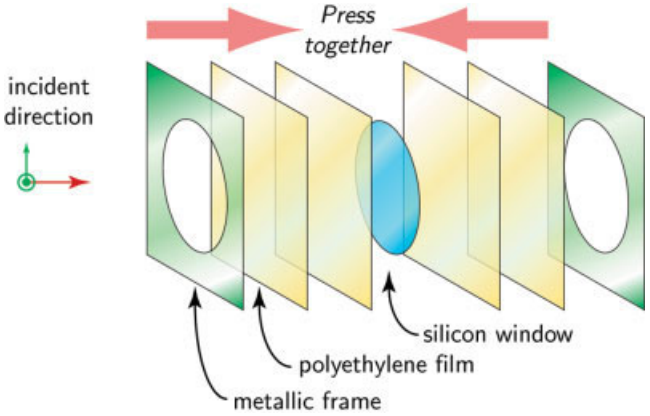

Figure 1 Retrofittable coating system. Multiple layers of polyethylene films are put together to achieve a required thickness, and pressed onto the silicon window by metallic frames. Combined together, these films perform as an antireflection coating for the silicon window. [Color figure can be viewed in the online issue, which is available at www.interscience.wiley.com]

In order to permit rapid change of a coating layer, a polyethylene film is stuck to a window by a supporting frame without adhesion, as demonstrated in Figure 1. Changing the coating thickness is simply carried out by replacing or adding polyethylene films.

In this article, the antireflection performance is verified for two different coating thicknesses, 48 ± 2.3 μm and 103 ± 10 μm. The thicker layer is composed of two polyethylene sheets, one has the thickness of 48 ± 2.3 μm and the other the thickness of 55 ± 7.6 μm. The same coating is applied to both sides of the silicon window. According to the quarter-wave formula, and assuming the index of refraction of polyethylene is 1.5, the thin coating would be optimized for a central frequency, where the reflectance is zero, at 1.04 THz, and the thick coating would be for a central frequency at 0.49 THz.

Prior to testing for the transmittance of the coated windows, the optical properties of bulk materials, that will be used for the window and coating, are measured separately, as they might possess some uncommon features induced by their production processes.

Supplied by *Siltronix*, the silicon window used in this experiment is undoped, ⟨100⟩, CZ-grown, polished on both sides, with the thickness of 1.5213 ± 0.0021 mm and the diameter of 10.2 cm. Through THz-TDS, the optical constants in the frequency range from 0.2 to 1.0 THz can be found, as shown in Figure 2.

Two low-density polyethylene films, taken from common PE bags, with the total thickness of 95.9 ± 4.6 μm are put together and measured for the optical constants in the T-ray frequency range. Figure 3 shows the index of refraction and the absorption coefficient of polyethylene.

Finally, the window coated by the PE films is measured for its transmittance. The transmittances of thinly-coated and thickly-coated windows are shown in Figures 4 and 5, respectively, in comparison with the transmittance of an uncoated window.

In the range of 0.7–1.0 THz, the thinly- or thickly-coated window shows a lower transmittance than that of the uncoated

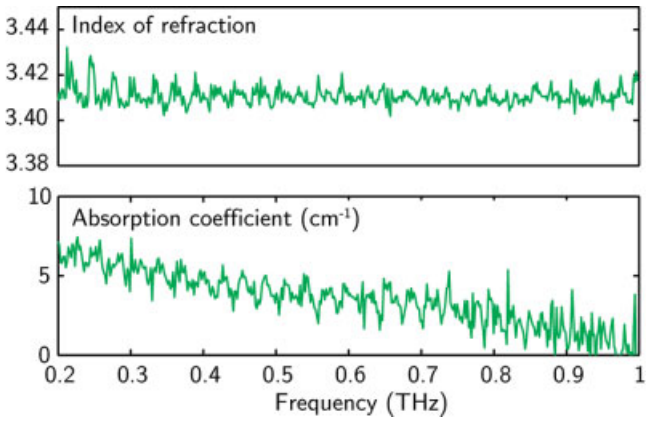

Figure 2 Optical constants of silicon. The index of refraction is constant over frequencies of interest, whereas the absorption coefficient is high at low frequencies. [Color figure can be viewed in the online issue, which is available at www.interscience.wiley.com]

window, because of the intrinsic absorption of the polyethylene sheets, which becomes large in this frequency range (see Fig. 3). The high absorption of polyethylene prevents observation of the antireflection performance between 0.7 and 1.0 THz.

For the thinly-coated window, the transmittance in Figure 4 has an enhancement, broadly from 0.3 to 0.6 THz, peaking at 0.45 THz. The peak transmittance position is in contradiction with the theoretical central frequency at 1.04 THz. For the thickly-coated window, the spectrum in Figure 5 shows two transmittance enhancements at 0.3 and 0.6 THz. Again, these positions conflict with the expected central frequency at 0.49 THz and its odd harmonic at 1.47 THz. Although the coating thickness variations are taken into consideration, the uncertainties in central frequency are not large enough to justify the measured results.

4. COMPARISON OF MEASURED RESULTS TO MODELS

A possible reason is that air gaps might be present between the coatings and the window, since no adhesive or vacuum is applied between them. (Note that our polyethylene sheets cannot support a vacuum.) In order to confirm this assumption, the characteristic

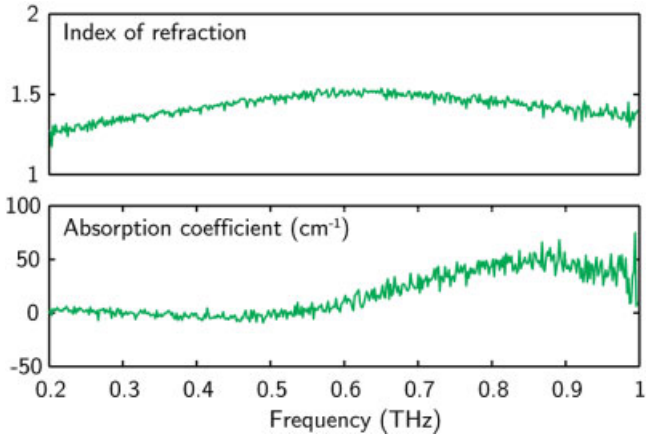

Figure 3 Optical constants of polyethylene. The index of refraction varies strongly with the frequency. The absorption coefficient is small from 0.2 to 0.5 THz, and increases rapidly after 0.5 THz. [Color figure can be viewed in the online issue, which is available at www.interscience.wiley.com]

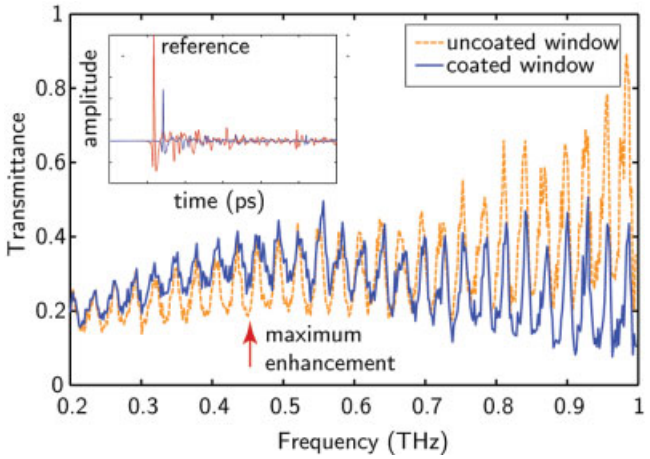

Figure 4 Measured transmittance of thin coating. The coated silicon window shows maximum transmittance enhancement at 0.45 THz. The inset shows the reference pulse and the pulses passing uncoated and coated windows. [Color figure can be viewed in the online issue, which is available at www.interscience.wiley.com]

matrix method is employed to simulate situations where narrow air gaps exist between the thin or thick coating and the window.

Figure 6 compares the calculated and measured transmittances of the thinly-coated window. In the simulation, two air gaps are set between the front and back coatings and the window, and the optical constants of silicon and polyethylene are taken from the measurement. The thicknesses of air gaps are varied in steps until the calculated transmittance is close to the measured transmittance. The theoretical thickness of each air gap is found to be around 45μm. The remaining discrepancies might be a result of thickness variation of silicon wafers and polyethylene sheets.

Similarly, for the thick coating case, four air gaps are assumed between the four polyethylene sheets and the window. The simulation gives the closest transmittance when the gap thickness is 65 μm (figure not shown here).

The transmittances calculated from the characteristic matrix method confirm that the implemented retrofittable antireflection system contains air gaps between the window and the coating.

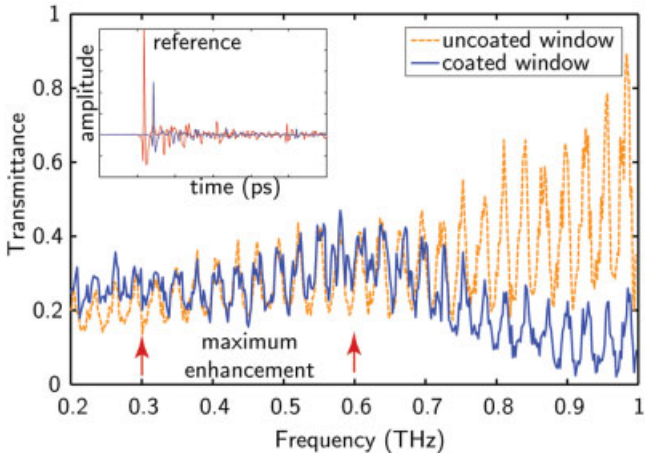

Figure 5 Measured transmittance of thick coating. The coated silicon window shows maximum transmittance enhancement at 0.3 and 0.6 THz. The inset shows the reference pulse and the pulses passing uncoated and coated windows. [Color figure can be viewed in the online issue, which is available at www.interscience.wiley.com]

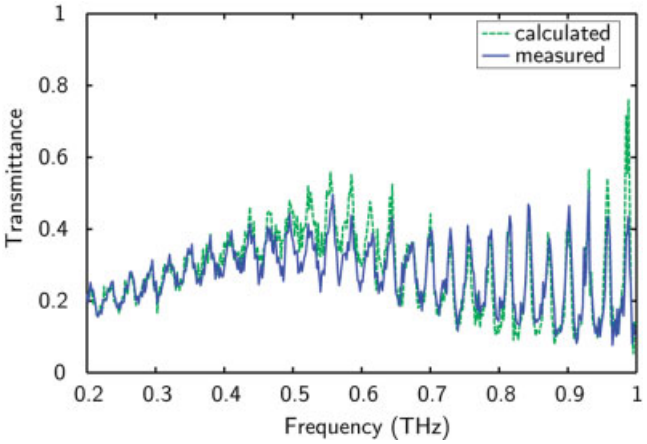

Figure 6 Calculated and measured transmittances of the thinly-coated silicon window. Two air gaps, each of which has the thickness of 45 μm, are inserted between the coatings and the window in the calculation. [Color figure can be viewed in the online issue, which is available at www.interscience.wiley.com]

Though the antireflection is still effective, its operational frequencies are offset from the designed frequencies.

5. CONCLUSION

In conclusion, the retrofittable antireflection coating system for a transmission window operating with T-rays has been demonstrated. The retrofittable system allows rapid interchange of the coating thickness and coating material to accommodate desired frequencies. In the experiment, a silicon wafer was selected as window coated by two thicknesses of polyethylene sheets. Even though the index of refraction of polyethylene coating was not perfectly suited to the silicon window, the coating enhances the window transmittance to a promising degree. However, the operational frequencies of the coating are different from theoretical expectation. Through a characteristic matrix analysis, it was found that air gaps present between the coatings and the window can explain the discrepancy. These air gaps, although difficult to remove, could probably be controlled in such a way to promote multilayer antireflection coatings.

REFERENCES

1. D. Grischkowsky, S. Keiding, M. van Exter, and Ch. Fattinger, Far-infrared time-domain spectroscopy with terahertz beams of dielectrics and semiconductors, J Opt Soc Am B 7 (1990), 2006–2015.
2. S.A. Harmon and R.A. Cheville, Part-per-million gas detection from long-baseline THz spectroscopy, Appl Phys Lett 85 (2004), 2128–2130.
3. C.R. Englert, M. Birk, and H. Maurer, Antireflection coated, wedged, single-crystal silicon aircraft window for the far-infrared, IEEE Trans Geosci Rem Sens 37 (1999), 1997–2003.
4. I. Hosako, Antireflection coating formed by plasma-enhanced chemical-vapor deposition for terahertz-frequency germanium optics, Appl Opt 42 (2003), 4045–4048.
5. E. Hecht, Optics, Addison-Wesley, London, 1987.

DETERMINING TRANSMISSION ZEROES OF THE GENERAL CHEBYSHEV FILTER

Qing-Xin Chu and Zhi-Hong Tu
School of Electronic and Information Engineering, South China University of Technology, Guangzhou 510640, China

Received 13 February 2007

ABSTRACT: *Determining transmission zeroes is the important precondition in the synthesis of the cross-coupled filter. A novel method to determine the general Chebyshev filter degree and transmission zeroes at the same time is proposed, according to the extreme characteristic of the general Chebyshev function and the relationship between the filter degree and the number of transmission zeros. On the condition of given filter specifications, the least filter degree and the optimum positions of transmission zeroes are realized. Several application examples illustrate the procedure and the validity of the proposed method.* © 2007 Wiley Periodicals, Inc. Microwave Opt Technol Lett 49: 2270–2275, 2007; Published online in Wiley InterScience (www.interscience.wiley.com). DOI 10.1002/mop.22663

Key words: *general Chebyshev function; cross-coupled filter; transmission zeros; transmission extreme frequency*

1. INTRODUCTION

RF filter is the fundamental element of the RF front of the wireless communication system. With the development of wireless communication, the more crowded the spectrum is, the more stringent specifications for designing filers are, especial for rectangularity. These specifications have become harder to be met by conventional Butterworth and Chebyshev filters. Now it is cross-coupled filters with finite transmission zeros that the best choices are, which are carried out by the general Chebyshev function. Compared with conventional filters, it can not only meet specifications, but also reduce the number of resonating elements and this, in turn, reduces the insertion loss, size, and manufacturing cost of the design. But it is more complicated to synthesis and design than conventional filters.

A general theory of cross-coupled filters was advanced by Atia and Williams in the 1970s, which was limited to the symmetric response filter with on complex equalization zeroes [1–2]. And later it was extended to the general case of asymmetric self-equalized filter by Cameron, possibly with multiple input/output couplings and direct coupling between the source and the load [3–5]. Cameron also gave a scheme to obtain a coupling matrix through extracting successively element values in a fix sequence from the lowpass prototype ABCD transmission matrix. The process went on until all resultant ABCD polynomials have zero degree [6–7]. The method of directly introducing a pair of transmission zeroes on the basis of low-pass Chebyshev filter and the CT/CQ filter synthesis were developed by Levy and coworkers [8–10]. In addition, optimization methods have shown to be an effective option to synthesize cross-coupled filters. A simple cost function along with a standard unconstrained gradient optimization technique was reported [11]. And later, Amari advanced an analytical expression for the gradient of the scattering parameter without recourse to the concept of the adjoin network for optimization [12].

All of methods above are the foundation of synthesizing advanced cross-coupled filters. But the precondition of these methods is that the filter degree and transmission zeroes must be prescribed. There are still few papers which deal with how to extract the filter degree and transmission zeroes. The common solution for deter-